Lattice Disorder and Size-Induced Kondo Behavior in $CeAl_2$ and $CePt_{2+x}$

S.-W. Han,[1,2] C. H. Booth,[2] E. D. Bauer,[3] P. H. Huang,[4] Y. Y. Chen,[4] and J. M. Lawrence[5]

[1]*Chonbuk National University, Jeonju, 561-756, Korea*

[2]*Chemical Sciences Division, Lawrence Berkeley National Laboratory, Berkeley, California 94720, USA*

[3]*Los Alamos National Laboratory, Los Alamos, New Mexico 87545, USA*

[4]*Institute of Physics, Academia Sinica, Taipei, Taiwan, Republic of China*

[5]*Department of Physics, University of California, Irvine, California 92697, USA*

(Dated: December 23, 2003, Version 1.5)

Abstract

When the particle size of $CeAl_2$ and $CePt_{2+x}$ samples is reduced to the nanometer scale, antiferromagnetism is suppressed and Kondo behavior dominates. X-ray absorption fine-structure measurements of the local Ce and Pt environments show that the nanoparticles are contracted relative to bulk samples. Although this implies an increase in the average Kondo temperature, the observation of additional disorder indicates that some fraction of f moments will remain unquenched even at very low temperatures. These results suggest that such nanoparticles, which already have the largest measured effective carrier masses, have the potential to generate far greater mass enhancements.

PACS numbers: 72.15.Qm, 61.10.Ht, 71.23.-k, 61.46.+w

$CeAl_2$, $CePt_2$ and $CePt_{2.5}$ have recently been shown to display the fascinating property that as their particle size becomes comparable to the nanometer scale, they change from displaying Kondo behavior above an antiferromagnetic (AF) transition (T_N = 3.9 K for $CeAl_2$ [1–7] and 1.6 K for $CePt_{2+x}$ [8–11]) to displaying only a nonmagnetic, Kondo ground state [12, 13]. The suppression of the magnetic ground state in the nanoparticles is thought to be due to the inability of small particles to support spin waves [12], as related to spin fluctuations in these materials [5–7]. Although particle size likely plays an important role in determining these physical properties, structural changes between the bulk and nanoscale particles may also play an important role. For instance, both the Kondo and Ruderman-Kittel-Kasuya-Yosida (RKKY) interactions depend strongly on the f/c (c=conduction electron) hybridization strength, V_{fc}, which in turn is a strong function of the nearest-neighbor environment around the Ce atoms. Therefore, lattice distortions or disorder could play an equally important or even dominating role compared to particle size in determining both distributions of interactions and even whether or not the ground state is magnetic.

To clarify these structural issues, we report x-ray absorption fine structure (XAFS) measurements on nanoparticles of $CeAl_2$, $CePt_2$ and $CePt_{2.5}$ and their bulk counterparts at the Ce and Pt $L_{\rm III}$-edges. Information about pair distances, coordination numbers and pair-distance distribution widths of near-neighbors from the absorbing atomic species indicate that large distortions and other disorder exist in each of these materials in their nanoparticle phase. By using a tight-binding form for V_{fc}, we demonstrate how these distortions couple to the magnetic properties with unexpected results, raising the possibility of extremely-heavy-fermion behavior.

The sample preparation methods are described elsewhere and the average particle size of the nanocrystals is 8.0 ± 0.5 nm in diameter for $CeAl_2$ [12] and 3.8 ± 0.3 nm for $CePt_2$ and $CePt_{2.5}$ samples, as determined by high-resolution transmission electron microscopy. AF is observed at 3.8 K, 1.7 K and 1.0 K, respectively, in the bulk starting material. The nanoparticle materials display no AF, but do display an enhanced linear coefficient of the specific heat. The values for $C_{\rm el}/T = \gamma \approx 7$, 0.6, and 0.2 J mol^{-1} K^{-2}, respectively, place these materials well within the criterion of heavy-fermion compounds. In fact, the value for $CeAl_2$ is currently the largest measured for any compound.

The samples were reground for XAFS measurements and passed through a 20 μm sieve. The sieved powder was spread uniformly over adhesive tape, cut into strips, and stacked to

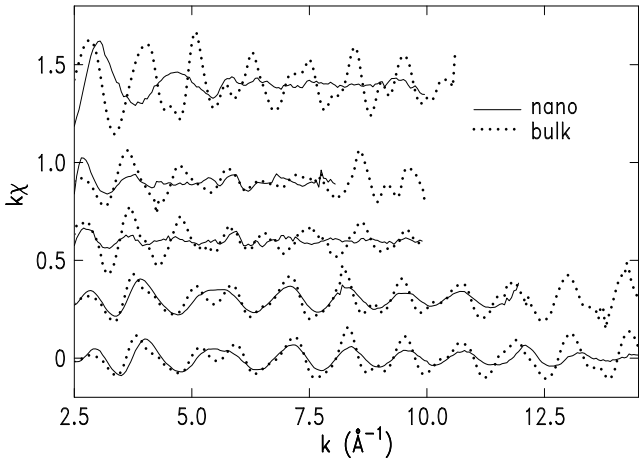

FIG. 1: XAFS ($k\chi$) as a function of wave number vector k measured at 20 K. From top, Ce $L_{\rm III}$-edge on $CeAl_2$, $CePt_2$ and $CePt_{2.5}$, and Pt $L_{\rm III}$-edge on $CePt_2$ and $CePt_{2.5}$. The XAFS data could not be obtained beyond $k = 10$ Å^{-1} at Ce $L_{\rm III}$-edge due to the Ce L_{II}-edge.

obtain samples with absorption edge steps corresponding to between $0.3 - 1.0$ absorption lengths. Transmission Ce and Pt $L_{\rm III}$-edge (5724 and 11564 eV, respectively) XAFS measurements on $CeAl_2$ and $CePt_{2.5}$ were made on beamline 2-3 at the Stanford Synchrotron Radiation Laboratory (SSRL) using a half-tuned Si(111) double-crystal monochromator. Data were collected on $CePt_2$ at the PNC-CAT of the Advanced Photon Source (APS) using a quarter-tuned Si(111) double-crystal monochromator.

XAFS data were analyzed with the UWXAFS package [14] using standard procedures [15] and photoelectron back-scattering functions calculated with the FEFF8 code [16]. After the atomic background absorption μ_0 was determined, the XAFS function $\chi = \mu/\mu_0 - 1$ was obtained. Figure 1 shows the XAFS from both the Ce and Pt $L_{\rm III}$ edges for all three samples as a function of the photoelectron wave vector $k = \sqrt{\frac{2m_e}{\hbar^2}(E - E_0)}$, where m_e is the electron rest mass, E is the incident photon energy and E_0 is the edge energy, chosen arbitrarily at the half-height of the edge. The weak intensity of the data from the nanoparticles indicates that their local structures are considerably disordered compared to their bulk counterparts.

Figures 2 and 3 show the magnitude of Fourier transformed (FT) XAFS data from bulk and nanocrystalline samples of $CeAl_2$ and $CePt_2$. FT data for $CePt_{2+x}$ are similar to the $CePt_2$ transforms. Note that the peaks are shifted on the $\tilde{r}$ axis from their true bond lengths due to the phase shift of the back scattered photoelectron. Detailed fits are therefore necessary to obtain quantitative information. Fits to the bulk data start from the $C15$ Laves

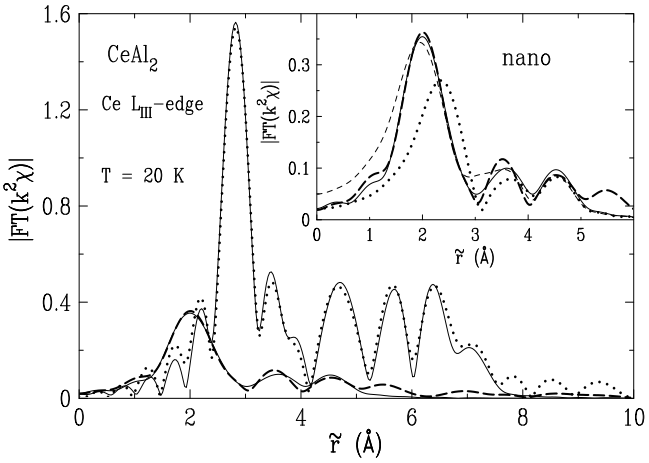

FIG. 2: Magnitude of Fourier transformed XAFS data from a bulk (dotted line) and a nanocrystal (thick-dashed line) of $CeAl_2$ as a function of distance from probe atom Ce. Solid lines are best fits. Inset indicates the XAFS data from the nanoparticle $CeAl_2$ and fits with the different models of Al-O mixed (solid line), Al only (dotted line) and O only (thin-dashed line). Ce $L_{\rm III}$-edge data are either transformed between $2.7 - 7.5$ Å^{-1} (nanocrystals) or $2.5 - 9.5$ Å^{-1} (bulk), with a Hanning window of width 0.5 Å^{-1}.

structure (space group $F\bar{4}3m$), allowing the bond lengths and the variance of the bond length distributions (σ^2, includes thermal vibrations and static disorder) for each shell below 7 Å to vary. The immediate environment around the Ce atoms on the $4a$ and $4c$ sites consists of 12 Al or Pt nearest neighbors on the $16e$ sites arranged in a regular icosahedron, closely followed by 4 Al or Pt atoms. The Al and Pt atoms sit on a corner-shared tetrahedral network, such that the local environment consists of 6 nearest-neighbor Al or Pt's followed by 6 Ce's at a somewhat longer distance. Note that the $CePt_{2.5}$ samples nominally have Pt on 1/7th of the $4a$ and $4c$ sites. The amplitude fractions for all pairs are held fixed to the nominal values in the fits to the bulk data. Fit quality for bulk samples is high, and the number of necessary fit parameters is well below the number of degrees of freedom, as estimated by Stern's rule [17]. The fit results are summarized in Table I. The small measured σ^2's for bulk $CeAl_2$ indicate that its crystalline structure is well ordered. The bulk σ^2's for the $CePt_{2+x}$ samples indicate some disorder exists even in the starting material. In any case, the measured local pair distances agree well with the average structures derived from diffraction measurements [6, 8, 18].

The nanoparticle fits start from the bulk model. Reliable results could not be obtained

for the Ce-Ce or more distant shells in $CeAl_2$ nanoparticles. In addition, reasonable fits could not be obtained without including at least one more shell compared to those used for the bulk data fit. The inset to Fig. 2 shows various fits assuming that (1) only aluminum, (2) only oxygen, and (3) both Al and O occur within the nearest-neighbor environment. The first two models do not fit the measured data satisfactorily. The fit is considerably improved by including about $1.2 \pm 0.6\%$ oxygens at a distance of about 2.44 Å, along with the main Ce-Al pairs at 2.96 Å. The Ce-O amplitude is consistent with about 15% CeO_2, although the Ce-O bond length is somewhat larger than the bulk value of 2.34 Å [19]. This observation of oxygen contamination agrees with the original study [12]. The situation is similar for the $CePt_{2+x}$ nanoparticles. The fits are not sensitive to Pt-O contamination or Ce-O in further shells within about 20%, nor were they sensitive to Ce/Pt site interchange beyond the nominal concentrations within about 12%.

In any case, the average σ^2 of the Ce-Al and Ce-Pt pairs is much larger and their pair distances are about considerably shorter than that of the same pairs in the bulk samples. Ce-Ce pairs all show a smaller contraction, but also show a large amount of disorder in the nanoparticles. Note that the same Ce-Pt pair distance is measured from the Pt L_{III} edge. Also note that the number of neighbors in the nanoparticles is similar to the bulk value, although the error bars are quite large beyond the nearest-neighbors. On the one hand, these measurements indicate that both large distortions and intrinsic disorder exist around Ce in the nanocrystals compared to the bulk. On the other hand, the basic structure still seems to be describable as a Laves phase. Interestingly, the Pt-Pt pairs contract only slightly in the bulk, and all the contractions are nearly to the limit set by the metallic radii of the constituent atoms [19]. If the structure really has remained in, approximately, a Laves phase, then the Ce atoms have likely been displaced off the center of the Al or Pt icosahedron. In such a case, the measured pair distance would be dominated by the shortest near-neighbor pairs. A cumulant analysis [20] to search for a skewed pair-distance distribution was, however, inconclusive.

The effect of all these distortions and the additional disorder on the magnetic properties of the nanoparticles can be calculated using a Kondo disorder model [21] in the same manner as has been applied to some non-Fermi liquid materials [22]. This model starts with a form for the Kondo temperature $T_{\mathrm{K}} = E_{\mathrm{F}} \exp(-1/(\rho V_{fd}^2/\epsilon_f)$, where E_F is the Fermi energy, ρ is the density of states at the Fermi level, and ϵ_f is the f-level energy. The following discussion

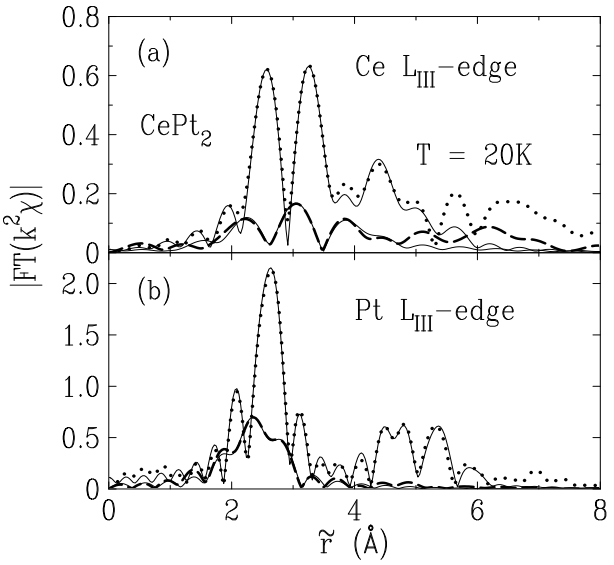

FIG. 3: Magnitude of Fourier transformed XAFS data from a bulk (dotted line) and a nanocrystal (thick-dashed line) of $CePt_2$ as a function of distance from probe atom Ce (a) and Pt (b). Solid lines are best fits. Ce data are transformed as in Fig. 2. Pt data are transformed between 2.5 − 14.5 Å^{-1} (bulk) or 2.5 − 11.5 Å^{-1} (nanocrystals) with a Hanning window of width 0.5 Å^{-1} was used.

is only semi-quantitative, since we assume that $E_{\rm F}$, ρ and ϵ_f are the same between the bulk and the nanoparticles, which is almost certainly not the case. If one considers a tight-binding form for the f/c hybridization energy [23] with d conduction electrons, X-shell radii r_X, constant η (see Appendix B in Ref. [23], assuming σ-bonds) and pair distance R_{fc},

$$V_{fc} = \sum_{\rm bonds} \frac{\eta_{fd}\hbar^2}{m_e} \frac{\sqrt{(r^5_{Ce\ f} r^3_{X\ d})}}{R^6_{Ce-X}}, \tag{1}$$

then V_{fc} will *increase* nearly 50% merely from the measured distortions. Assuming a relatively low value for $\rho/\epsilon_f \approx 1$ eV^{-2}, such an increase will increase $T_{\rm K}$ by about 270% (see Fig. 4). However, the effective $T_{\rm K}$ is observed to *decrease* from about 5 K to 0.7 K from heat capacity measurements of $CeAl_2$. Moreover, the lattice spacing, although difficult to estimate from x-ray diffraction data due to particle-size broadening, appears to expand, in agreement with the observed decrease in $T_{\rm K}$. These apparent contradictions to the XAFS results are explained by considering the effect of the additional observed disorder. We note here that the nature of this disorder is not quantifiable by these data. That is, it is entirely possible that the enhanced σ^2's are due to a distribution of distortions that relates to the

TABLE I: Fit results for all measured samples at 20 K. A single value of S_0^2 and ΔE_0 was used for each sample at each edge. The nanoparticle value for S_0^2 was fixed to the value from the bulk sample. The number of fit parameters is well below the number of independent data points as estimated with Stern's rule [17]. Bond lengths and σ^2's in $CePt_2$ and $CePt_{2.5}$ determined at Ce and Pt L_{III}-edges at 20 K

			Bulk Sample			Nanoparticle Sample		
	pair	S_0^2	N	r(Å)	σ^2(Å^2)	N	r(Å)	σ^2(Å^2)
$CeAl_2$	Ce-Al	0.90(6)	12	3.356(5)	0.0038(4)	11(2)	2.96(2)	0.044(9)
	Ce-Ce		4	3.503(6)	0.0021(7)			
	Ce-O					1.2(6)	2.44(3)	0.006(4)
$CePt_2$	Ce-Pt	0.85(10)	12	3.18(1)	0.012(1)	11(1)	2.91(1)	0.025(2)
	Ce-Ce		4	3.43(1)	0.002(1)	3.8(6)	3.37(1)	0.017(3)
	Ce-O					1.5(6)	2.50(5)	0.025(9)
	Pt-Pt	0.83(5)	6	2.723(2)	0.0015(2)	6.4(5)	2.690(5)	0.0051(2)
	Pt-Ce		6	3.19(1)	0.013(1)	6(1)	2.86(2)	0.048(8)
$CePt_{2.5}$	Ce-Pt	0.95(10)	12	3.18(1)	0.014(1)	10.8(10)	2.84(1)	0.021(1)
	Ce-Ce/Pt[a]		4	3.44(2)	0.003(1)	3.9(5)	3.29(1)	0.024(2)
	Ce-O					1.6(3)	2.39(3)	0.020(6)
	Pt-Pt	0.85(7)	36/7	2.713(2)	0.0019(2)	6.1(6)	2.690(3)	0.0056(3)
	Pt-Ce/Pt[a]		36/7	3.13(1)	0.014(1)	5.5(9)	2.92(3)	0.034(5)

[a] 6/7th of N are Ce, 1/7th are Pt, R constrained to the same value, σ^2's constrained by the ratio of the reduced masses.

particle size distribution. Keeping this in mind, we make a rough estimate of this distribution with a Gaussian distribution of pair-distances, as in the XAFS fits. Including such a distribution in Eq. 1, we obtain the broad distribution of V_{fc} shown in Fig. 4. Note that this distribution extends far below the bulk value. Although this distribution is only a rough estimate and given the aforementioned assumptions, even if it extends only to 0.4 eV, then the T_K distribution would extend down to ~0.07 K. If this part of the distribution could be isolated, then one could imagine γ's on the Clearly, the huge width of the V_{fc} distribution will likely dominate the effect on the distribution of T_K's.

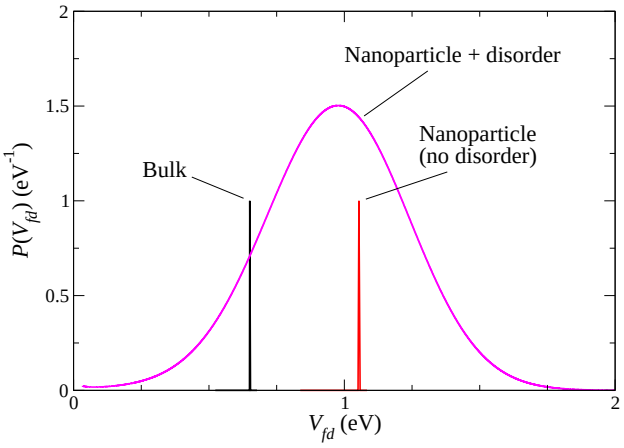

FIG. 4: The f-electron/conduction electron hybridization energy V_{fc} distribution for $CePt_2$ assuming the measured pair distances (actually δ-functions), and the measured disorder in the Ce-Pt pairs. See text for details.

In summary, we have studied the local structural properties of nanocrystalline $CeAl_2$, $CePt_2$ and $CePt_{2.5}$ compared with their bulk counterparts. A substantial amount of disorder in the nanoparticles is observed and the Ce−Al and Ce−Pt bond lengths are significantly shorter than that in the bulk. Although the effect of these changes is strongly dependent on the microscopic details of the disorder, such structural changes will have a dominating effect on the magnetic properties, and hence should be included in any proper theory of the changes in the physical properties of nanocrystalline $CeAl_2$, $CePt_2$ and $CePt_{2.5}$.

This work is supported in part by the Office of Science, U.S. Department of Energy (DOE) under contract No. DE-AC03-76SF00098. The data of $CeAl_2$ and $CePt_{2.5}$ were collected at the Stanford Synchrotron Radiation Laboratory, a national user facility supported by the US DOE and Office of Basic Energy Sciences(OBES). $CePt_2$ data were taken at Advanced Photon Source at Argonne National Laboratory supported by the US DOE, OBES.

[1] B. Barbara, J. X. Boucherle, J. L. Buevoz, M. F. Rossingnol, and J. Schweizer, Solid State Commun. **24**, 481 (1977).

[2] B. Barbara, M. F. Rossingnol, J. X. Boucherle, J. Schweizer, and J. L. Buevoz, J. Appl. Phys. **50**, 2300 (1979).

[3] K. H. J. Buschow and H. J. van Daal, Phys. Rev. Lett. **23**, 408 (1969).

[4] D. E. MacLaughlin, O. Pẽna, and M. Lysak, Phys. Rev. B **23**, 1039 (1981).

[5] M. Croft, I. Zoric, and R. D. Parks, Phys. Rev. B **18**, 345 (1978).

[6] M. Croft and H. H. Levine, Phys. Rev. B **22**, 4366 (1980).

[7] M. Croft and H. H. Levine, Phys. Rev. Lett. **46**, 1104 (1981).

[8] J. M. Lawrence, Y.-C. Chen, G. H. Kwei, M. F. Hundley, and J. D. Thompson, Phys. Rev B **56**, 5 (1997).

[9] A. B. Andrews, J. J. Joyce, A. J. Arko, J. D. Thompson, J. Tang, J. M. Lawrence, and J. C. Hemminger, Phys. Rev. B **51**, R3277 (1995).

[10] L. Rebelsky, K. Reilly, S. Horn, H. Borges, J. D. Thompson, and R. Caspary, J. Appl. Phys. **67**, 5206 (1990).

[11] R. R. Joseph, J. K. A. Gschneidner, and R. E. Hungsgerg, Phys. Rev. B **5**, 1878 (1972).

[12] Y. Y. Chen, Y. D. Yao, C. R. Wang, W. H. Li, C. L. CHang, T. K. Lee, T. M. Hong, J. C. Ho, and S. F. Pan, Phys. Rev. Lett. **84**, 4990 (2000).

[13] Y. Y. Chen, Y. D. Yao, C. R. Wang, W. H. Li, C. L. CHang, T. K. Lee, T. M. Hong, J. C. Ho, and S. F. Pan, study of x-ray absorption near edge structure, heat capactiy and magnetic susceptibility on $CePt_{2+x}$ compounds.

[14] E. A. Stern, M. Newville, B. Ravel, Y. Yacoby, and D. Haskel, Physica B **208 & 209**, 117 (1995), find further information of UWXAFS at http://depts.washington.edu/uwxafs.

[15] S.-W. Han, E. A. Stern, D. Haskel, and A. R. Moodenbaugh, Phys. Rev. B **66**, 094101 (2002).

[16] A. L. Ankudinov, B. Ravel, J. J. Rehr, and S. D. Conradson, Phys. Rev. B **58**, 7565 (1998).

[17] E. A. Stern, Phys. Rev. B **48**, 9825 (1993).

[18] W. H. Zachariasen, Acta. Cryst. **2**, 388 (1949).

[19] R. W. G. Wyckoff, *Crystal Structures* (Interscience Publishers, New York, 1964), 2nd ed.

[20] P. Eisenberger and G. S. Brown, Solid State Commun. **29**, 418 (1979).

[21] O. O. Bernal, D. E. MacLaughlin, H. G. Lukefahr, and B. Andraka, Phys. Rev. Lett. **75**, 2023 (1995).

[22] E. D. Bauer, C. H. Booth, G. H. Kwei, R. Chau, and M. B. Maple, Phys. Rev. B **65**, 245114 (2001).

[23] W. A. Harrison and G. K. Straub, Phys. Rev. B **36**, 2695 (1987).